MHD-PIC simulations of impurity transport by ELMs

D.C. van Vugt[1], G.T.A. Huijsmans[2,1], L.P.J. Kamp[1], A. Loarte[3], N.J. Lopes Cardozo[1]

[1] *Eindhoven University of Technology, Eindhoven, The Netherlands*

[2] *CEA, IRFM, F-13108 St. Paul Lez Durance, France*

[3] *ITER Organization, F-13067 St. Paul Lez Durance, France*

Abstract

A combined MHD-Particle in Cell model is used to study tungsten impurity transport during ELMs. Electromagnetic forces and particle streaming in ergodic fields have been found to drive particle flushing. Up to 20% of the particles in the pedestal region and nearly 3% of the impurities inside the separatrix are expelled in 500 μs.

Introduction

For stable tokamak operation the accumulation of heavy impurities in the plasma core must be prevented. Disruptions and radiative collapse could be triggered when the fraction of tungsten (W) in the core plasma reaches 10^{-4}. The core W density depends on production at the divertor, transport into the core plasma and flushing by ELMs. The production of W has a large contribution [1] during ELMs due to the enhanced heat and particle flux. The ELMs can also influence impurity transport and flush impurities from the core plasma [2, 3]. It is therefore an open question whether ELMs ultimately have beneficial or detrimental effects, which depends on the efficiency of impurity flushing. This we will therefore investigate. Impurity flushing can be caused by a number of effects, including a local $E \times B$ flow, charge state change during particle orbits, neoclassical temperature gradient forces or a combination of the parallel flow with an ergodized magnetic field.

In this work we present an extension of the MHD code JOREK [4], suitable for simulating impurity transport during ELMs. It combines a state-of-the-art MHD solver with a kinetic particle-in-cell model. This model features full-orbit tracking of impurities in the electromagnetic fields present during an ELM, as calculated by JOREK. A model for ionization, recombination and radiation is implemented, based on OPEN-ADAS data.

Simulations of impurity transport in MHD fields

Since there can be many different kinds of impurities, some with a large gyroradius it is advantageous to use a kinetic model. To follow the impurities we then have to integrate the equation of motion. For this, we use the well-known Boris-Buneman method [5, 6]. There are several other processes influencing the impurities, such as collisions, ionization and recombination. We model the ionization and recombination processes with rates from the OPEN-ADAS ADF11 database. Collisional effects have not yet been implemented.

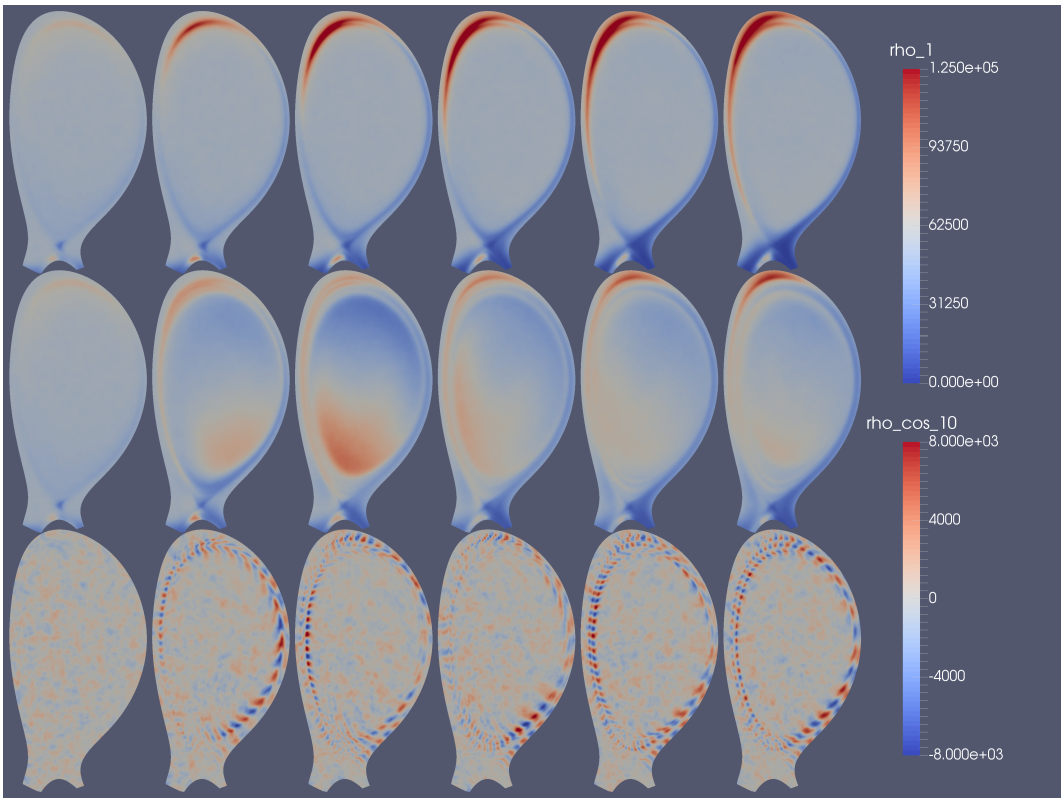

Figure 1: Projection of particles onto JOREK basis functions in the equilibrium case (top) and during an ELM (symmetric, middle and on the $n = 10$ mode, bottom) at time intervals of 130 microseconds. Color indicates particle number density. Initial density is 5.3×10^4 m^{-3}.

The fields acting upon the particle are obtained by coupling with the non-linear MHD code JOREK [4]. Particles are initialized uniformly throughout the plasma, with velocities sampled from the local temperature distribution. The charge state is calculated from a coronal equilibrium model. This initialization method still needs work, as it does not produce a steady-state impurity distribution.

These particles are followed throughout the growth phase and crash of the instability in a JET-like geometry. The ELM energy loss is 186 kJ, or 6% of the energy content inside the separatrix. Figure 1 shows the tungsten impurity profile at intervals of 130 microseconds. The profile has a significant toroidally symmetric component and a component with the $n = 10$ periodicity of the simulated ELM. To compare with the situation without an ELM also the symmetric component of the equilibrium case has been shown.

Tungsten impurities in ELMs

An initial test of the model with tungsten is performed here, with a rough comparison to carbon impurity flushing experiments.

It is instructive to look at the flux-surface averaged impurity density. In figure 2 these have been plotted for both the ELM and $n = 0$ case at intervals of 130 microseconds.

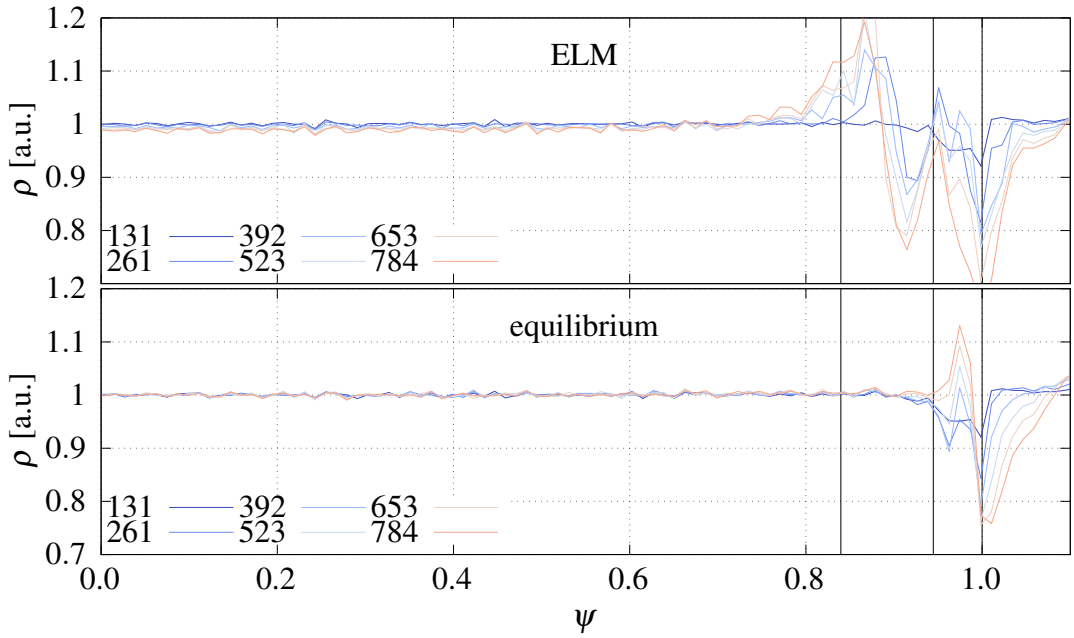

Figure 2: Tungsten density versus normalized flux coordinate ψ (zero at core, one at separatrix) at different times (in microseconds) during an ELM. The black lines represent the new density pedestal, the old density pedestal and the separatrix from left to right. Features of interest are the lowering of the impurity density near the pedestal and the increase near $\psi = 0.88$.

The edge impurity density can be seen to decrease, while a peak forms further inside the pedestal.

A timetrace of the impurity density versus the flux coordinate is shown in figure 3. The onset of the ELM is clearly visible, as well as the accumulation of impurities between $\psi = 0.8$ and $\psi = 0.9$. There has been little difference observed in the overall behaviour when including ionization and recombination, therefore only the ionizationless case is shown. The location of particle loss corresponds to experimental results [3]. The total number of particles inside the separatrix decreases with roughly 3% during the ELM. The plasma density decreases by 2% in the same period. The edge impurity density decreases much faster however, losing 20% in the edge region in 500 μs.

Future work

There are several avenues of investigation possible. The first is the improvement of the initial condition of the impurity ions. To validate against existing experiments of ELM impurity flushing this must be accurately reproduced. The implementation and validation of the collision model will be an important step towards this goal. In that case an accurate initial distribution can be obtained by injecting impurities at a similar location as in exper-

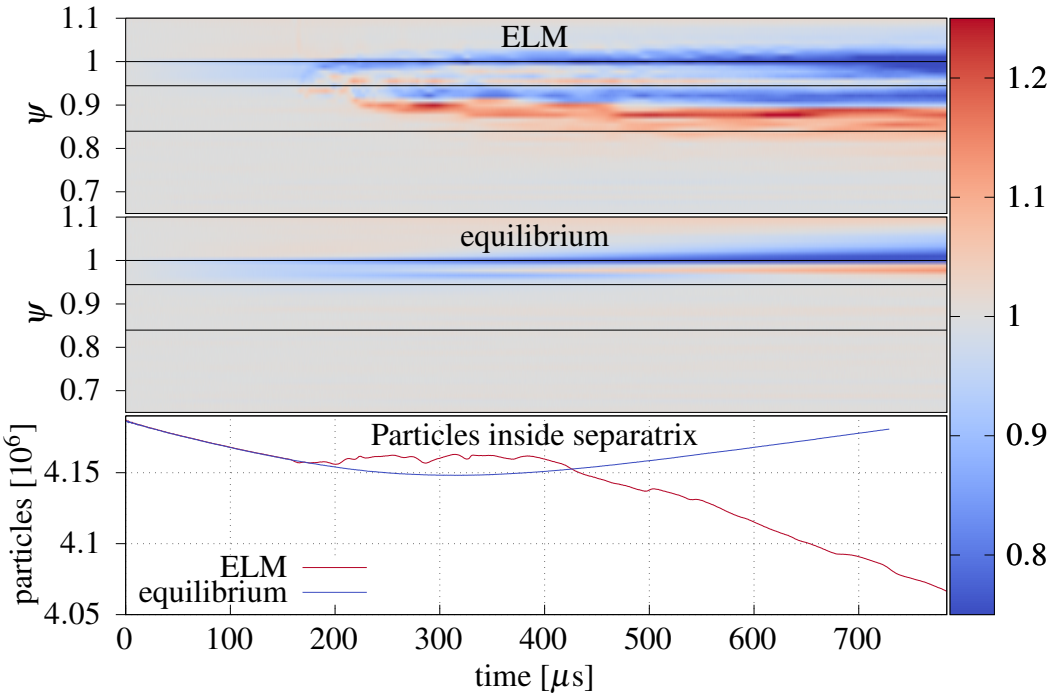

Figure 3: Tungsten density ρ during an ELM (top graph) and during an equivalent equilibrium calculation (middle graph). Only electromagnetic forces are taken into account. The time-variation in the $n = 0$ case is due to the particle initialization. The black lines represent the separatrix, the old density pedestal and the new density pedestal from top to bottom.

iments. The region of validity of the model can then be extended towards the divertor, to eventually simulate impurity production from sputtering.

To understand the causes of impurity flushing it is interesting to look at the role of the electric field, and at the regions in phasespace that lose many particles.

Improvement of the statistics in the model can be done by increasing the number of macroparticles, but perhaps also by using low-discrepancy series for the particle initialization in phase space.

The model can readily be used to simulate the behaviour of trace impurities in other situations such as during sawteeth and in the QH-mode.

References

[1] N. Den Harder et al. In: *Nucl. Fusion* 56.2 (2016), p. 026014.

[2] D. L. Hillis et al. In: *J. Nucl. Mater.* 196-198.C (1992), pp. 35–44.

[3] M. R. Wade et al. In: *Phys. Rev. Lett.* 94.22 (2005), pp. 1–4.

[4] G.T.A. Huysmans and O. Czarny. In: *Nucl. Fusion* 47.7 (2007), pp. 659–666.

[5] J. P. Boris. In: *Proc. Fourth Conf. Num. Sim. Plasmas*. 1970, pp. 3–67.

[6] O. Buneman. In: *J. Comput. Phys.* 1.4 (1967), pp. 517–535.